TNF-α inhibits glucocorticoid receptor-induced gene expression by reshaping the GR nuclear cofactor profile

Karen Dendoncker[a,b,1], Steven Timmermans[a,b,1], Jolien Vandewalle[a,b], Melanie Eggermont[a,b], Joanna Lempiäinen[c], Evelien Van Hamme[d], Sylviane Dewaele[a,b], Sofie Vandevyver[a,b], Marlies Ballegeer[a,b], Jolien Souffriau[a,b], Lise Van Wyngene[a,b], Kelly Van Looveren[a,b], Tineke Vanderhaeghen[a,b], Rudi Beyaert[a,b], Karolien De Bosscher[e,f], Jorma J. Palvimo[c], Marc Van Montagu[g,h,i,2], and Claude Libert[a,b,2]

[a]Mouse Genetics in Inflammation, VIB Center for Inflammation Research, 9052 Ghent, Belgium; [b]Department of Biomedical Molecular Biology, Ghent University, 9052 Ghent, Belgium; [c]Institute of Biomedicine, University of Eastern Finland, 70211 Kuopio, Finland; [d]Bio Imaging Core, VIB Center for Inflammation Research, 9052 Ghent, Belgium; [e]Medical Biotechnology Center, VIB, 9000 Ghent, Belgium; [f]Department of Biochemistry, Ghent University, 9000 Ghent, Belgium; [g]Department of Plant Biotechnology and Bioinformatics, Ghent University, 9052 Ghent, Belgium; [h]Center for Plant Systems Biology, VIB, 9052 Ghent, Belgium; and [i]International Plant Biotechnology Outreach, VIB, 9052 Ghent, Belgium

Contributed by Marc Van Montagu, May 5, 2019 (sent for review December 18, 2018; reviewed by Carme Caelles, Jin Mo Park, and Lienhard Schmitz)

Glucocorticoid resistance (GCR) is defined as an unresponsiveness to the therapeutic effects, including the antiinflammatory ones of glucocorticoids (GCs) and their receptor, the glucocorticoid receptor (GR). It is a problem in the management of inflammatory diseases and can be congenital as well as acquired. The strong proinflammatory cytokine TNF-alpha (TNF) induces an acute form of GCR, not only in mice, but also in several cell lines: e.g., in the hepatoma cell line BWTG3, as evidenced by impaired Dexamethasone (Dex)-stimulated direct GR-dependent gene up- and down-regulation. We report that TNF has a significant and broad impact on this transcriptional performance of GR, but no impact on nuclear translocation, dimerization, or DNA binding capacity of GR. Proteome-wide proximity-mapping (BioID), however, revealed that the GR interactome was strongly modulated by TNF. One GR cofactor that interacted significantly less with the receptor under GCR conditions is p300. NFκB activation and p300 knockdown both reduced direct transcriptional output of GR whereas p300 overexpression and NFκB inhibition reverted TNF-induced GCR, which is in support of a cofactor reshuffle model. This hypothesis was supported by FRET studies. This mechanism of GCR opens avenues for therapeutic interventions in GCR diseases.

transcription | regulation | genetics | mechanism

Glucocorticoids (GCs) regulate a wide variety of processes, including metabolic homeostasis, cell proliferation, inflammation, and immune responses (1). Synthetic GCs, such as dexamethasone (Dex), are often used to treat inflammatory disorders, such as asthma (2) and rheumatoid arthritis (RA). They exert their functions by binding to their intracellular receptor, the glucocorticoid receptor (GR) (3). Upon ligand binding, the GR translocates to the nucleus where it acts as a monomeric or dimeric transcription factor (TF) and regulates an extensive set of genes (4). As a homodimer, the GR binds to glucocorticoid responsive elements (GREs) in upstream regions of direct GC/GR up-regulated, as well as down-regulated, genes. These GRE sequences form variations of a 15-bp consensus sequence consisting of two imperfect palindromic hexamers separated by a 3-bp spacer (5). GR monomers are also able to bind DNA directly, on half GRE sites (6), and can also regulate expression of certain genes in a direct way, but GR homodimerization has appeared as the dominant GR configuration leading to direct gene regulation by GR. Many of these insights have followed from studies using the GRdim mutant mice, which express a poorly dimer-forming GR (7) and by recent genome-wide ChIP studies (6). Genes that are controlled by direct GR gene regulation include antiinflammatory genes, such as *Dusp1* (encoding MKP-1) and *Tsc22d3* (encoding GILZ) (5).

Besides this mechanism, GR can also influence gene expression by interacting with other transcription factors, such as AP1 and NF-κB (8), a process mainly performed by GR monomers. Finally, GR can also regulate gene expression by binding to several types of negative GRE elements (e.g., inverted repeat negative GREs) (9) in upstream regions of GC-responsive genes, such as *Stat1*, and inhibit their transcription (10). GC-mediated regulation of genes is associated with the recruitment of transcriptional coregulators, such as the p160 steroid receptor coactivator (SRC) family (11), and chromatin remodeling factors, as well as p300 histone acetyl transferase (12) and corepressors.

Despite the excellent antiinflammatory efficacy of GCs, their therapeutic use can be hampered by the onset of adverse effects, such as osteoporosis (13). Glucocorticoid resistance (GCR) is another major drawback. GCR is defined as a poor response to

Significance

Millions of patients suffer from inflammatory diseases and are treated by synthetic glucocorticoids as a first-line medication, but many become resistant after a certain period or display a lack of response to the treatment. The inflammatory cytokine TNF has been shown to be an important inducer of glucocorticoid resistance (GCR) against the antiinflammatory effects of glucocorticoids. We found an aspect of the GCR mechanism that specifically involves the sequestration of a transcriptional cofactor p300 by the inflammatory transcription factor NFκB, precluding accessibility to the glucocorticoid receptor (GR). Our data suggest that selective increase of the p300 availability for GR, but not for NFκB, may prevent or revert the problem of GCR and improve the glucocorticoid therapeutic value in inflammation.

Author contributions: K.D., S.T., R.B., M.V.M., and C.L. designed research; K.D., S.T., J.V., M.E., J.L., E.V.H., S.D., S.V., M.B., J.S., L.V.W., K.V.L., T.V., and C.L. performed research; R.B., K.D.B., J.J.P., M.V.M., and C.L. contributed new reagents/analytic tools; S.T., E.V.H., M.B., R.B., K.D.B., J.J.P., M.V.M., and C.L. analyzed data; and K.D., S.T., and C.L. wrote the paper.

Reviewers: C.C., University of Barcelona; J.M.P., Massachusetts General Hospital and Harvard Medical School; and L.S., University of Giessen.

The authors declare no conflict of interest.

Data deposition: The data reported in this paper have been deposited in the Gene Expression Omnibus (GEO) database, https://www.ncbi.nlm.nih.gov/geo (accession nos. GSE123953 and GSE124088).

[1]K.D. and S.T. contributed equally to this work.

[2]To whom correspondence may be addressed. Email: marc.vanmontagu@ugent.be or claude.libert@irc.VIB-UGent.be.

This article contains supporting information online at www.pnas.org/lookup/suppl/doi:10.1073/pnas.1821565116/-/DCSupplemental.

Published online June 10, 2019.

the therapeutic effects of GCs. Since GCs are also essential in first-line treatment of certain cancers, such as acute lymphocytic leukemia (ALL), GCR goes beyond a problem with the antiinflammatory effects of GCs. In rare cases, patients can be GCR based on a congenital, inheritable problem with the function of GR, but usually GCR is acquired (12). The incidence of GCR depends on the disease and ranges from a few percent of patients with asthma, to about 30% in RA and inflammatory bowel disease, to almost 100% in chronic obstructive pulmonary disease (COPD) and sepsis (14). The mechanism of GCR is far from clear and needs further investigation (15, 16).

Tumor necrosis factor (TNF) is an important player in many inflammatory diseases. It exerts its biological functions via interaction with two membrane receptors, TNFR1 and TNFR2 (17), which activate intracellular events that result in the activation of TFs, including NFκB and AP1 via TNF receptor-associated factor 2 (TRAF2) (18, 19). Upon TNF stimulation, the IκB kinase (IKK) complex is activated (20), leading to phosphorylation and ubiquitination of IκB, the inhibitor of NFκB and proteasomal degradation. This allows NFκB to translocate to the nucleus and to initiate transcription via binding of predominantly NFκB dimers p50 and p65 to κB sites, found in many proinflammatory genes. The p50/p65 transcription factor attracts numerous cofactors to initiate transcription. The inflammatory effects of TNF are manifested in the release of a wave of proinflammatory cytokines, such as IL-6 and IL-1β (21), which precede cell death, inflammation, and organ damage.

TNF plays a prominent role in the development of GCR, as suggested previously (22–24). We have reported that TNF compromises the protective antiinflammatory function of GR against lethal inflammation in mice (25), which we consider thus as a TNF-induced specific form of GCR. TNF also induces GCR in cell systems, including the lung epithelial cell line A549 (26). In recent studies, we have shown that GR homodimerization is absolutely essential in sustaining a basal protection, as well as in mounting antiinflammatory protection by exogenous, pharmacological synthetic GCs, in a model of acute, lethal inflammation (10). The data underline the importance of direct gene regulation by GR dimers. In the current study, we investigated the underlying mechanism of TNF-induced GCR and have focused on the impact of TNF on direct Dex-induced gene regulation. We propose that GCR is a result of a dynamic reshaping of the GR nuclear cofactor profile and suggest that the exchange of the multifunctional cofactor p300 between GR and NFκB is essential in this process.

Results

TNF Pretreatment Induced a State of GCR In Vivo and In Vitro. Mice were first injected with PBS or TNF, and, 4 h later, they were injected with 100 μg of Dex, and, 2 h later, GR inducible genes (GRE genes) were measured. In mice pretreated with PBS, Dex transcriptionally up-regulated several well-known GR-inducible genes in the liver (PBS/Dex vs. PBS/PBS) (*SI Appendix*, Fig. S1 *A–E*). When mice had been pretreated with TNF, none of the four GRE genes could be transcriptionally up-regulated by Dex (TNF/Dex vs. TNF/PBS). Then, cellular systems for GCR were developed. Three cell lines, the human A549 and HEK293T cells and mouse BWTG3 cells, were transiently transfected with a GRE-luc reporter construct and stimulated. Since HEK293T cells have no endogenously active GR, they were transfected with a human GR cDNA as well. Throughout this study, different treatment regimen were used: namely, (*i*) medium [noninduced (NI)], (*ii*) 1 μM Dex for 2 h, (*iii*) TNF 1,000 IU/mL for 3 h, (*iv*) 1 h TNF pretreatment followed by Dex 2 h (TNF/Dex) without TNF washout, so a total of 3 h TNF incubation. The analyzed GRE-luciferase monitored the transcriptional gene up-regulating the GR activity. A significant induction was seen of GRE-luciferase upon Dex stimulation and TNF-induced GCR in all three lines (*SI Appendix*, Fig. S1 *F–H*).

To obtain a genome-wide perspective of GCR, an RNA-sequencing (RNA-Seq) analysis was performed in BWTG3 cells (27). This mouse hepatoma line was selected because of the importance of hepatocytes in acute inflammation, because the liver is a TNF-responsive organ, and because of the high expression levels of GR in these cells (25). To detect differences in gene regulation, expression values were analyzed by pairwise fold-change comparisons. They were calculated by comparing the relative expression after stimulation. The four stimulation conditions mentioned before were applied. We only considered genes up- or down-regulated at least twofold [log fold change (LFC) of 1 or −1], and, using a false discovery rate (FDR) of 5%, we found that Dex (compared with NI) significantly induced 802 genes and significantly reduced the expression of 119 genes. The 802 and 119 genes are listed in *SI Appendix*, Table S1. One hundred sixty-six of the 802 genes were significantly changed (up or down) by a single TNF incubation, compared with the NI condition. The remaining 636 genes are thus directly Dex-induced but unaffected by TNF alone. In this group of 636 genes, we found that a majority of 481 genes (76%) attained significantly lower expression levels after TNF/Dex of at least 20%, compared with NI versus Dex to NI. The Venn diagram in Fig. 1*A* illustrates these findings. Very similarly, of the 119 direct DEX–down-regulated genes, 104 were unaffected by TNF alone. Of these 104 genes, 75 (72%) were significantly and at least 20% less down-regulated, compared with NI, by TNF/Dex compared with Dex (Fig. 1*B*).

The broad, generic effect of TNF on this direct GR transcriptional activity was supported by the hierarchical clustering analysis (heat map, *SI Appendix*, Fig. S2). These data illustrate that the TNF/Dex condition clusters closer to the TNF condition than to the Dex condition. When the LFCs of the 636 genes for Dex and TNF/Dex were compared in a plot, the slope r of the linear regression curve ($r = 0.036 \pm 0.015$) was significantly different from 1 (Fig. 1*C*). Fig. 1*D* illustrates that the relative impact of TNF pretreatment on the transcriptional output of the 636 Dex-induced genes was very strong. Similar data were obtained when studying the 104 Dex–down-regulated genes (Fig. 1*E*). In a genome-wide perspective (*SI Appendix*, Table S1), the numbers of Dex-induced and Dex-reduced genes showing a complete block by TNF were 416 resp. 69 genes, while the numbers of genes escaping significant TNF impact were 155 resp. 29. Examples of Dex-induced genes displaying a complete GCR (e.g., *Psca*, *Slc26a9*, and *Eci2*) are shown in Fig. 1*F*. Since most of the differentially regulated genes are up-regulated by Dex, and based on compelling evidence suggesting that dimer-dependent direct GR gene regulation exhibits marked antiinflammatory properties (5, 10, 28), we further focused on the effect of TNF on key points in the direct GR gene up-regulating pathway.

TNF Pretreatment Did Not Affect Nuclear Translocation or GR Dimerization. Most GR-mediated gene regulatory activities occur in the nucleus, and GR nuclear translocation precedes GR-regulated gene induction. BWTG3 cells were treated with the four conditions. Using Western blot analysis of cytoplasmic and nuclear fractions (*SI Appendix*, Fig. S3 *A* and *B*) and indirect immunofluorescence analysis (*SI Appendix*, Fig. S3*C*), we found that Dex stimulation induces nuclear import of GR. When BWTG3 cells were pretreated with TNF, Dex-induced GR nuclear translocation remained functional, with equal protein levels detected in the nucleus after Dex stimulation in the absence or presence of TNF. Similar results were obtained in the GR-transfected HEK293T cells (*SI Appendix*, Fig. S3*D*). These data demonstrate that TNF pretreatment does not abrogate nuclear translocation of GR, and the data also exclude that TNF may lead to a significant GR degradation, as had been suggested earlier (25).

Since GR homodimerization is essential for GR's direct transcriptional activity that we were addressing in this study, we studied whether TNF pretreatment could decrease GR dimerization, which was investigated using fluorescence resonance energy transfer (FRET). HEK293T cells were transfected with plasmids encoding a CFP-tagged GR and a YFP-tagged GR. HEK293T cells were used for this purpose because they do not contain an

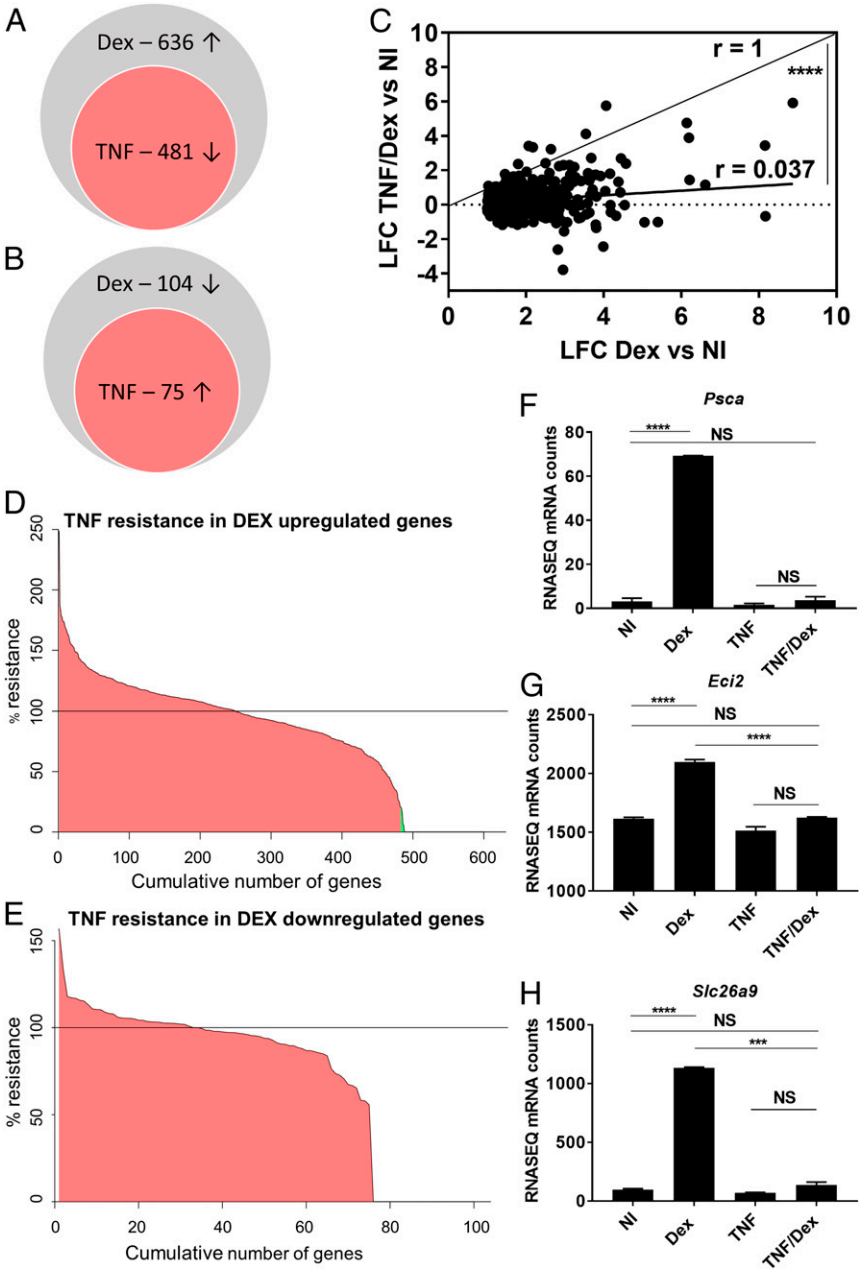

Fig. 1. Genome-wide study of TNF-induced GCR in BWTG3 cells via RNA sequencing. (*A*) Scheme indicating that 636 genes were up-regulated upon Dex stimulation, all of which were not modified by a TNF incubation only; 481 of these genes were significantly less induced by Dex, when cells were pretreated by TNF. (*B*) Similarly, scheme indicating that Dex down-regulated 104 genes, 75 of which were less reduced by TNF/Dex compared with Dex. (*C*) Plot of the LFCs of the inductions of 636 genes, induction by Dex-NI (horizontal axis) and by TNF/Dex-NI (vertical axis), followed by linear regression analysis. Slope of the curve is $r = 0.036 \pm 0.015$, which is highly significantly different from the diagonal curve with slope $r = 1$. (*D* and *E*) The cumulative number of genes in function of the degree of impact of TNF on their Dex regulation for Dex–up-regulated (*D*) and Dex–down-regulated genes (*E*). The genes in green are Dex-induced genes significantly reduced by TNF, but with an impact of TNF of less than 20%. (*F–H*) RNA-Seq–based counts of transcripts of several genes as examples of genes suffering from complete (*F–H*) GCR. Significances of *P* values are mentioned as $^{***}P < 0.001$, $^{****}P < 0.0001$, or NS (nonsignificant).

endogenous functional GR. Transfected HEK293T cells were treated with Dex, with or without 1-h TNF pretreatment, and FRET signals were analyzed in function of time, using confocal microscopy with Velocity software (*SI Appendix*, Fig. S3 *E* and *F*). The results confirm that Dex stimulation leads to GR dimerization and demonstrate that there is no impact of TNF on the pattern.

TNF Did Not Modulate GR-DNA Binding. We evaluated the impact of TNF on the DNA-binding capacity of GR by ChIP-Seq in BWTG3 cells treated with the four conditions (ref. 29; see *SI Appendix*, *Supporting Information Methods* for details). We found a total of 212 peaks in the NI condition, 5,693 peaks in the Dex condition, 936 peaks after TNF-only treatment, and 5,940 peaks after the TNF/Dex treatment. Regardless of TNF pretreatment, Dex led to the appearance of the GRE motif with the highest significance (*SI Appendix*, Fig. S4). In both Dex conditions, besides the GRE motif, also the FOXA1 motif was strongly enriched, with slightly less significance, but with even more genes displaying this motif. In the few peaks that were present in the NI condition, FOX:EBOX and Tcf4 were the top motives in terms of significance, and, in the TNF conditions, the top motifs were FOXA1, Tcf4, and BATF. In the Dex and TNF/Dex condition, GRE enrichment was more prominent in top scoring peaks. While over 30% of the total number of peaks contain a GRE element, this proportion increased to ∼55% when only the top 10% best peak regions were taken into consideration (*SI Appendix*, Fig. S5).

We next studied the potential differences of intensities of GR-DNA binding peaks between the four conditions, with a special attention for the Dex versus TNF/Dex conditions, using the diffbind R package. The union of the peaks in all conditions was used for this study. Significant differences were detected between NI and Dex (2,590 peaks) and NI and TNF/Dex (3,129 peaks). There were very few differences between the NI and TNF-only conditions in terms of peak intensities. There were also very few differences between the Dex and TNF/Dex conditions. This is illustrated in the scatter plots. In these plots, each point represents

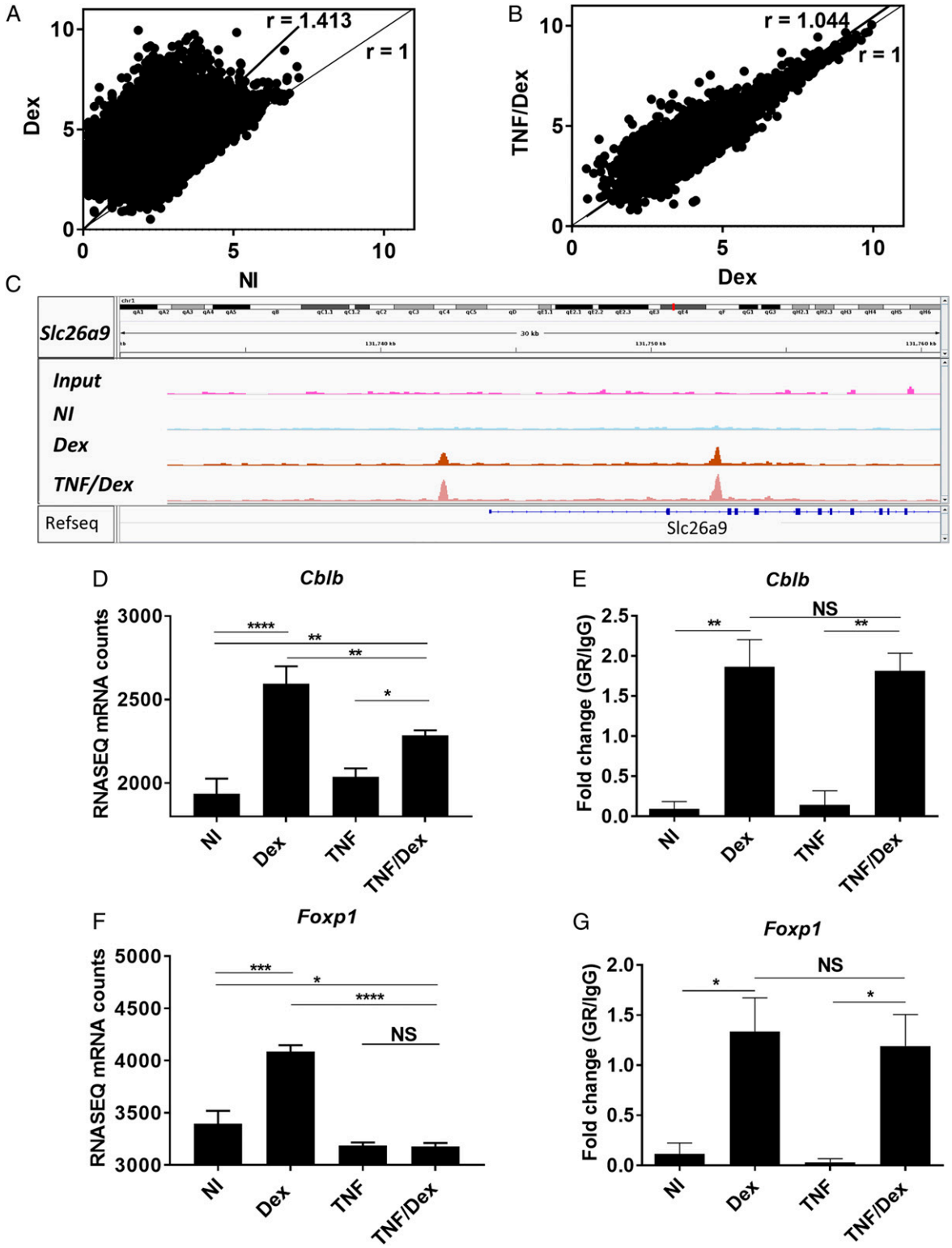

Fig. 2. TNF did not affect GR-DNA binding in BWTG3 cells. (*A* and *B*) Scatter plots of differences in peaks from the GR ChIP-Seq experiment. (*A*) Peak intensities of Dex-treated versus NI-treated cells. (*B*) Peak intensities of TNF/Dex versus Dex-treated cells. In both plots, linear regression was performed, resulting in a best-fitting curve, and the slope of the curve was calculated. (*C*) An example of specific GR peaks, associated with the Dex-induced gene *Slc26a9*, which underwent TNF-induced GCR and (*D*–*G*) RNA-Seq results ($n = 3$) and ChIP-qPCR results ($n = 4$) of two Dex-induced genes (*Cblb* and *Foxp1*), which underwent GCR. Significances of *P* values are mentioned as $^{*}P < 0.05$, $^{**}P < 0.01$, $^{***}P < 0.001$, $^{****}P < 0.0001$, or NS (nonsignificant).

the log2 (in both conditions) of the number of sequence reads under a peak region (thus the peak summits), with a fixed width. The NI vs. Dex comparison clearly showed a shift toward the Dex conditions (Fig. 2*A*), but, in the Dex vs. TNF/Dex comparison, most points were located on, or close to, the diagonal (Fig. 2*B*). By means of illustration, we show GR peaks distributed over the genome of a Dex-induced gene, that undergoes GCR by TNF in BWTG3 viz. *Slc26a9* (mRNA expression data) (Fig. 1). The ChIP-seq results were validated by specific ChIP qPCR experiments (Fig. 2 *D*–*G*) derived from an independent experiment in BWTG3 cells, for several genes (*Cblb* and *Foxp1*).

The GR Cofactor Profile Was Reshaped upon TNF Pretreatment. To regulate gene transcription after DNA binding, GR must attract and interact with transcriptional cofactors and coregulators. We investigated the GR interaction profile in GR-expressing HEK293T cells, by proteome-wide application of BioID. In this technique, a biotin ligase, BirA, was fused to the N-terminal part of GR, and the gene was stably integrated in the cells and expressed at physiological levels, enabling BirA biotinylation of proteins based on their proximity (30). This strategy has recently been shown to be particularly amenable for nuclear receptors such as the GR and androgen receptor (31).

The setup of the BioID strategy is shown in *SI Appendix*, Fig. S6. The BirA-GR fusion protein was expressed from a tetracycline-inducible stably integrated plasmid, and the experiment was run with BirA-GFP as a control in parallel. Cells were stimulated with the four conditions in quintuplicate. Fifty micromolar biotin was added to the cells together with Dex, and cells were harvested 6 h later and each sample analyzed in triplicate. Of note, in this setup, GR-expressing HEK293T cells were also susceptible to the TNF-induced GCR effects, as illustrated by the effects on a GRE-luciferase reporter (*SI Appendix*, Fig. S7).

Biotinylated proteins were isolated by streptavidin affinity capture and identified by mass spectrometry, and their original protein spectrum match (PSM) values were normalized to the bait (GR or GFP) PSM value in each sample. Candidate proteins were selected based on a procedure which harnesses a decision classification tree (*SI Appendix*, Figs. S6 and S8). Briefly, candidate GR interaction partners were selected if their CRAPome score (32) was below the arbitrary threshold of 80 and if their PSM value was at least two-times enriched compared with the GFP-BirA background. Additionally, GR partners were labeled "enriched after Dex stimulation" if their PSM in the Dex condition was at least twofold higher compared with the PSM in the TNF/Dex condition and vice versa.

When these criteria were applied, 423 GR interactions were found that were preferred in the Dex-only condition (Fig. 3*A*, in green), compared with the TNF/Dex condition. Hence, as a double criterion, proteins were enriched at least twofold over both background and TNF/Dex (i.e., Dex over ctrl >2 and Dex over TNF/Dex >2). Remarkably, only 57 proteins were shared in the Dex and the TNF/Dex condition (Fig. 3*A*, in blue). TNF pretreatment resulted in the formation of 197 specific interactions with GR (Fig. 3*A*, in red). The complete lists of these three groups of GR interaction partners are provided in *SI Appendix*, Table S5. A protein description search was performed using the UniProt database to rearrange the hits based on their function. The most appealing GR interaction partners in the three groups are shown in *SI Appendix*, Table S6, and the graphic display in Fig. 3*B* reveals that several subunits of the mediator complex, the FACT complex (facilitates chromatin transcription), Cdk1, and TAF2 (Transcription initiation factor TFIID subunit 2), were enriched to GR in the Dex-only condition compared with the TNF/Dex condition, suggesting that TNF interfered with RNA polymerase-driven transcriptional activation. Also, the histone acetyltransferase p300 was found to be 2.7 times more enriched with the GR upon Dex stimulation, compared with TNF/Dex. Reports have described a fundamental role for p300 in bridging nuclear receptors with RNA polymerase II (Pol-II) and in facilitating an "open" and accessible chromatin structure which allows gene transcription (33). Furthermore, p300 is necessary for GC signaling (34). In this respect, it would be conceivable that TNF reduced the interaction between p300 and GR and that the ensuing cofactor exchanges led to an inadequate RNA Pol-II assembly and function, with reduced direct GR transcriptional activity as a consequence.

P300 Plays a Crucial Role in Direct GR Gene-Inducing Activity. To support the link between GR-p300 binding and GCR, a ChIP analysis with an antibody against p300 was performed (in BWTG3 cells) to investigate the physical recruitment of p300 (the mRNA expression of which does not vary by any treatment of BWTG3 cells) to GRE genes. P300 was specifically observed at the GR-binding site (GBS) located upstream of the transcription start sites (TSSs) of the *Cblb*, *Eci2*, and *Per1* genes, after Dex treatment (Fig. 3 *C*, *D*, and *F*). The two former genes are typical Dex-induced genes which suffer from significant GCR (Figs. 1 and 2) while *Per1* does not show strong GCR (Fig. 3*E*) and displays convincing GR chromatin-binding peaks. Interestingly, the recruitment of p300 to the GBS of the GCR genes reduced significantly when cells were pretreated with TNF, but not so in the case of *Per1*. As a background control, p300 binding was not detected at the transcription start site of these genes. This finding illustrates that p300 was enriched at the GBS of these promoters in a Dex-dependent way and that this interaction was impaired in TNF-induced GCR.

To support the idea that p300 is functionally involved in the TNF-induced GCR, the effect of modulation of p300 concentrations on the GR transcriptional activity with and without TNF pretreatment was investigated in cells. First, p300 expression was knocked down, and the effect on GR function was studied. Since knockdown (KD) of the endogenous p300-coding gene (*Ep300*) was repeatedly unsuccessful in BWTG3 or HEK293T cells, we performed this experiment in A549 cells. A significant KD of about 50% on protein level was achieved (Fig. 4*A*). The effect of p300 depletion on selected GR-induced genes (stimulated by Dex) was validated with qPCR analysis of cells treated with and without Dex. The induction of the GRE genes *Fkbp5* and *Tsc22d3* (Fig. 4 *B* and *C*) was significantly reduced by p300 KD. This result confirms that p300 is essential for the regulation of GR target genes. Second, transient transfection of p300 in HEK293T cells, which significantly increases p300 mRNA and protein (Fig. 4*D*), had no impact on the induction of GR transcriptional activity after Dex stimulation, compared with a GFP gene transfection control (Fig. 4*E*). In sharp contrast, p300 overexpression reverted TNF-induced GCR. This finding suggests that, in normal conditions, sufficient (saturated) amounts of p300 were available for GR to achieve the appropriate transcriptional output and that, in TNF/Dex conditions, insufficient p300 was available for GR.

NFκB and GR Exchange p300. The most abundant TF-binding motifs of the TNF-induced genes in the BWTG3 RNA-Seq experiment were NFκB-p65-Rel and NFκB-p65 motifs followed by NFκB-p50 (Fig. 4*F*). Various cross-talk mechanisms between GR and the NFκB signaling pathways have been described before (35), and we hypothesized that p300 plays a key role in this interplay. p300 has already been shown to stimulate the activation of p65 and to acetylate p65 which enhances the p65-DNA binding (36).

We confirmed that p300 is essential in TNF-induced NFκB activation. We overexpressed p300 in GR-expressing HEK293T cells, stimulated the cells with TNF, and studied NFκB activity using a luciferase reporter. Clearly, p300 overexpression led to increased NFκB activation upon TNF treatment (Fig. 4*G*). We then investigated whether overexpression of proteins of different mediators of the NFκB activation pathway was sufficient to induce GCR to confirm the hypothesis that NFκB mediates TNF-induced GCR. Two different concentrations of TRAF2, IKKβ, and p65 plasmids were expressed in GR-expressing HEK293T

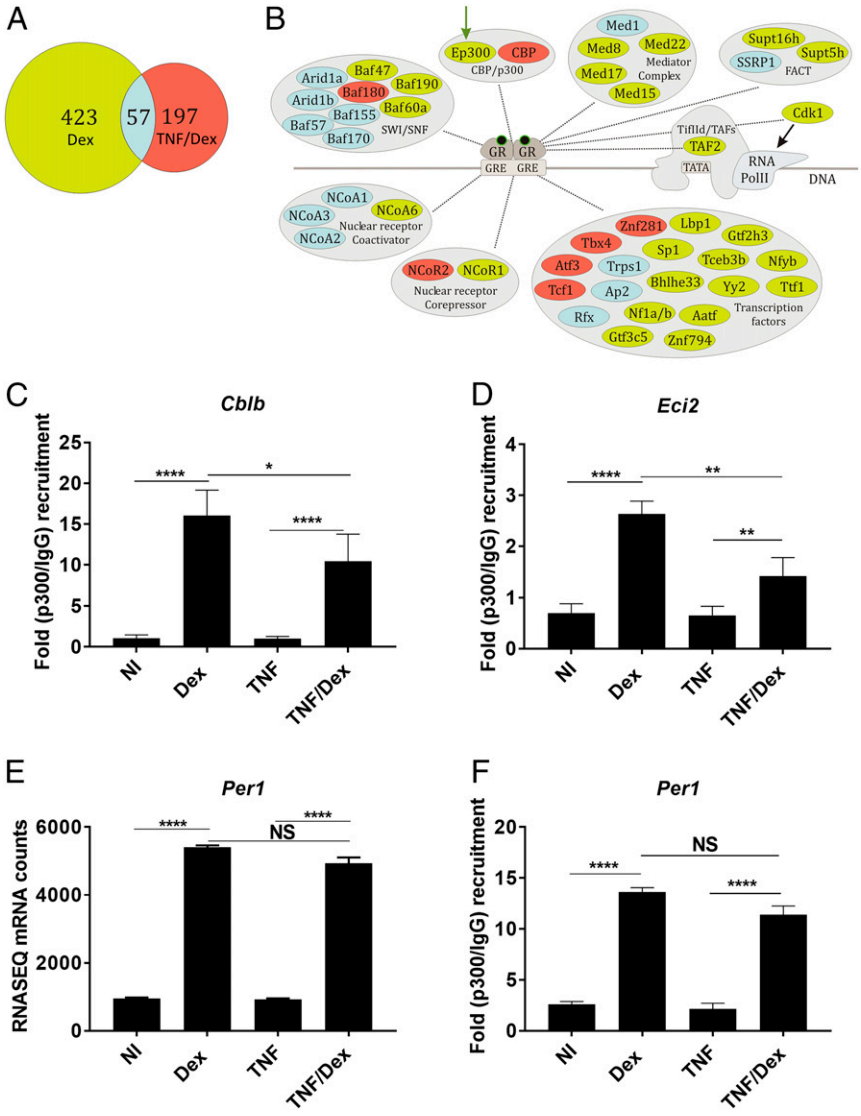

Fig. 3. Impact of TNF on GR interactome in Dex-stimulated HEK293T cells and p300 levels. GR interactome was studied by the BirA BioID technology. (*A*) Venn diagram showing that 423 GR-interacting proteins (green) were enriched in Dex-stimulated compared with TNF/Dex-treated cells (FC ≥ 2); 57 proteins (blue) were shared in the Dex and the TNF/Dex condition, and 197 GR-interactors appeared in the TNF/Dex treatment group (red). (*B*) GR-interacting proteins were clustered according to molecular function. (*C*, *D*, and *F*) p300 Chip-qPCR signals at GR-binding sites on *Cblb* and *Eci2* (two genes undergoing GCR) and *Per1*, a gene escaping significant GCR (*E*) 2 h after Dex stimulation. Results were normalized to input chromatin and are shown as the ratio of p300 recruitment vs. IgG control. Results shown are means ± SD ($n = 4$). Significances of *P* values are mentioned as $*P < 0.05$, $**P < 0.01$, $***P < 0.001$, $****P < 0.0001$, or NS (nonsignificant). FACT, facilitating chromatin transcription; SWI/SNF, switching defective/sucrose nonfermenting.

cells, as well as GFP cDNA as a control plasmid (Fig. 4*H*), and cells were stimulated with Dex, and the GR transcriptional activity was measured by GRE-luciferase expression. Overexpression of all three proteins was sufficient to cause significantly reduced transcriptional output by GR, compared with the GFP control. In this setup, several NFκB-induced genes were measured and indeed found to be induced by these three genes, to confirm the activity of the plasmids (*SI Appendix*, Fig. S9). Stably transfected A549 cells with the GRE-luc reporter construct were then exposed to 5 μM TPCA1, a specific IKK inhibitor, which prevented the TNF-induced GCR highly significantly (Fig. 4*I*), indicating that p65 is involved in the establishment of GCR.

Based on our data, we suggest a "first come, first serve" hypothesis in the establishing of GCR: In basal situations, sufficient but limiting amounts of p300 are available to serve GR or p65. Depending on which transcription factor is activated first, p300 is recruited to this particular TF to enhance transcription, leaving subsequently activated TFs with fewer p300. To support this hypothesis, we studied the GR-p300 interaction via FRET, using ECFP-GR– and EYFP-p300–coding plasmids in HEK293T cells. After transfection, cells were stimulated with the four conditions. As displayed in Fig. 5*A*, Dex stimulation led to significant GR-p300 FRET signals, and the TNF/Dex FRET signal was significantly (42%) lower than Dex-FRET signals, confirming the BioID result. Interestingly, the NFκB inhibitor TPCA1 eliminated the TNF effect (Fig. 5*B*), and p65 cotransfection along with GR and p300 significantly reduced the GR-p300 FRET signal (Fig. 5*C*).

In Vivo Prevention of GCR by p300 Overexpression. Finally, we investigated whether increasing the expression of p300 modulates TNF-induced reduction in GR transcriptional gene activation in vivo. To increase p300 expression, the expression plasmids coding for human p300 and GFP (see HEK293T experiment) were transiently transfected in livers of mice using hydrodynamic plasmid injection in the tail vein of mice (*Materials and Methods*), leading to a 30% increase in p300 protein after 24 h (*SI Appendix*, Fig. S10). After plasmid injection, mice were injected with 30 μg of TNF, and, 6 h later, Dex was injected. GR-dependent gene expression of *Tsc22d3*, *Dusp1*, and *Ddit4* was measured by RT-qPCR in livers, isolated 2 h after Dex injection (Fig. 5 *D*–*F*). The results revealed that, upon p300 overexpression, the fold impact of TNF on the gene induction by Dex is less severe. Hence, providing GR with more p300 in conditions of inflammation could be a considerable option in novel strategies to overcome GCR.

Discussion

TNF has been identified as an important mediator in the induction of GCR. Since the term GCR is also of relevance toward other

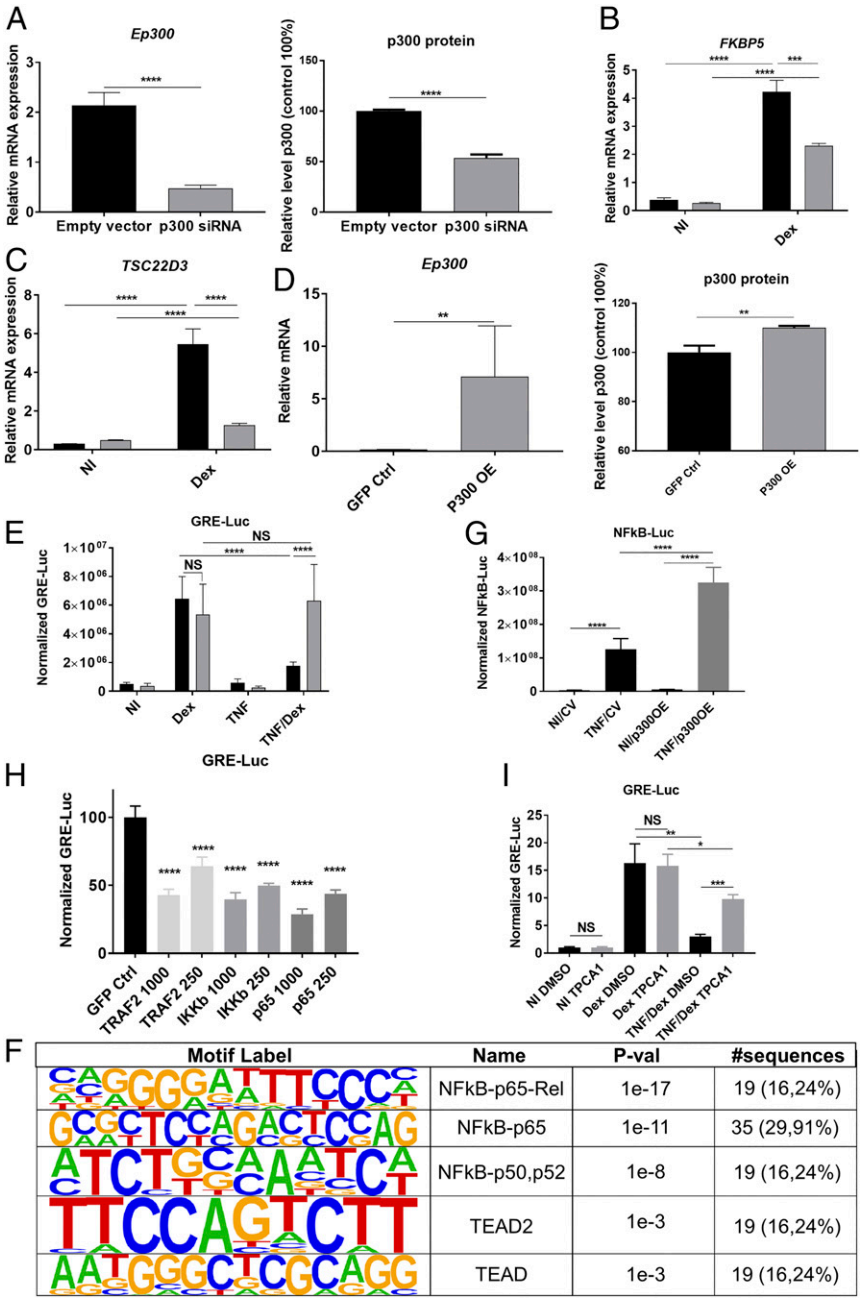

Fig. 4. P300 and NFκB are involved in TNF-induced GCR. (*A*–*C*) Impact of p300 knockdown on Dex response in A549 cells. (*A*) mRNA levels (qPCR) and protein levels (dot blot) analysis of p300 levels 24 h after transfection of A549 cells with a control vector or a p300-siRNA vector. (*B*) *FKBP5* and (*C*) *TSC22D3* gene induction levels (qPCR) in cells treated with control vector (black) or p300 siRNA vector (gray). Cells were treated with 1 μM Dex for 5 h or non-induced (NI). Data are shown as mean ± SD. (*D* and *E*) Impact of overexpression of p300 on GR transcriptional activity. (*D*) Impact of p300 overexpression (OE) in HEK293T cells on p300 mRNA (qPCR 24 h after transfection of a p300-expressing vector compared with a GFP-overexpressing vector [with same backbone and promoter)] and protein (dot blot) levels. (*E*) Effect of p300 overexpression on GRE-luciferase expression. HEK293T cells were transfected with GFP (black) or p300 (gray) and left untreated or treated for 2 h with 1 μM Dex with or without 1 h pretreatment with TNF. Data are shown as mean ± SD ($n = 3$). (*F*) HOMER motif analysis of the genes induced by TNF in the BWTG3 RNA-Seq experiment. (*G*) Luciferase activity in HEK293T cells transfected with GFP gene (black) or with p300 (gray) and stimulated, 24 h after transfection, with or without 1,000 U/mL TNF for 1 h. Data are mean ± SD ($n = 6$). (*H*) The effect of expression of three NFκB signaling proteins, TRAF2, IKKb, and p65 and GFP on the GRE-luciferase expression in HEK293T cells stimulated with 1 μM Dex for 5 h. Cells were transfected with 1,000 ng or 250 ng of plasmid. Data are means and SDs, and data were studied by one-way ANOVA with Dunnett's multiple comparison test ($n = 6$). (*I*) Impact of the NFκB inhibitor TPCA1 on TNF-induced GCR. Stable GRE-Luciferase–transfected A549 cells were stimulated with 5 μM TPCA1, 30 min before TNF pretreatment. Cells were then stimulated with the usual conditions, for 2 h. Values are averages of four technical replicates of three independent experiments. Data are mean ± SD studied by one-way ANOVA and Tukey's multiple comparison test ($n = 3$). Significances of *P* values are mentioned as $*P < 0.05$, $**P < 0.01$, $***P < 0.001$, $****P < 0.0001$, or NS (nonsignificant).

therapeutic applications of GCs (e.g., their anticancer effect in ALL or immune suppression), we here consider only GCR as an insufficient response to the antiinflammatory function of GCs. The levels of TNF or NFκB activation often correlate with the degree of GCR and the severity of the inflammatory disorder: e.g., in regions of the gut epithelium of patients with Crohn's disease where local GCR was strongly correlated with local MAPK and NFκB activation (37) and the expression of proinflammatory cytokines during inflammatory diseases is linked with GCR (38–40).

We here investigated the mechanism of how TNF induced GCR in vitro and how the GC sensitivity can be restored in vitro and in vivo. In mice, as well as in cell lines used in this study, TNF treatment consistently reduced the impact of Dex on direct transcriptional up-regulation and down-regulation of GRE genes. In our study, we have focused on direct GR–up-regulated and GR–down-regulated genes, involving direct binding of GR to DNA. As is supported by the motif analysis by the ChIP-Seq experiment and RNA-Seq experiment, this function of GR involved binding to full, canonical GRE elements and is very likely a GR dimer function. Based on our work using mice with poor GR dimerization capacity and their enormous sensitivity for inflammation and practically absent antiinflammatory protection by Dex (10), we focused this study on this direct type of GR gene regulation.

We found that the effect of TNF pretreatment on the genome-wide Dex-regulated transcriptome in BWTG3 cells was fast, strong, and broad. Not all genes directly induced or reduced by Dex were equally affected by TNF pretreatment. Some genes (about one quarter) even escaped GCR entirely: Right now, we can only speculate about the reason behind this observation. Assuming that p300 is the key determinant in GCR, as we suggest in this paper, some genes might be induced by the GR in a way that did not involve p300. In support of these notions, the reduction of p300 recruitment to GR as assessed by the GR-p300

FRET data was not complete, but was about 25 to 50%. Interestingly, the nature of GR binding sequences (GBSs) in the DNA not only functions as GR binding platforms, but also modulate the GR conformation and gene-specific regulatory activity of GR by the recruitment of a GBS sequence-specific cofactor profile. Hence, DNA acts as a sequence-specific ligand of GR to meet the specific needs of gene-dependent expression (41). The genes that escaped GCR form too small a family to find common motifs in the GRE elements that drive them and to conclude that these are genes that were induced without p300 as a cofactor. The case of the *Per1* gene illustrates that genes escaping GCR may be induced by GR, but that, at those genes, GR-p300 interaction is not influenced by TNF pretreatment. Hence, the titration of p300 from GR may show gene-specific effects that will be addressed in future studies.

In this paper, we suggest that a shift in cofactor recruitment was the main cause for the reduced direct GR gene up-regulation and gene down-regulation activity. When considering the broad effect on GR during GCR as a loss of function or recruitment of RNA Pol-II, the underlying mechanism may well have involved a cofactor issue. The application of the BioID technology in Dex-stimulated BirA-GR–expressing HEK293T cells treated with and without TNF was successful in identifying interaction partners of GR in a proteome-wide, albeit not gene-specific, way. In total, more than 2,700 biotinylated proteins were identified by mass spectrometry. Hundreds of proteins were found to be recruited significantly less to GR by Dex in TNF-pretreated cells, and almost 200 proteins were significantly more recruited to GR under these circumstances. SRC-2 has been shown to restore GC responsiveness in airway epithelium (42), but, in our study, the three major GR cofactors belonging to the p160 SRC family, including SRC-1 (NCoA-1), SRC-2 (NCoA-2, GRIP-1, TIF2), and SRC-3, were, however, not modulated by TNF.

Most cofactors are thought to perform multiple functions including chromatin reorganization, histone modification and formation of scaffolds that allow recruitment of more cofactors and attracting members of the Mediator complex and regulate RNA polymerase II (Pol-II) recruitment and activity. There were several reasons why we focused our attention on the histone/lysine acetyltransferase p300 as a GR partner. First, p300 has been shown to contribute to GR-mediated transcription (34), as well as to the activities of other transcription factors (43), including NFκB (p65)

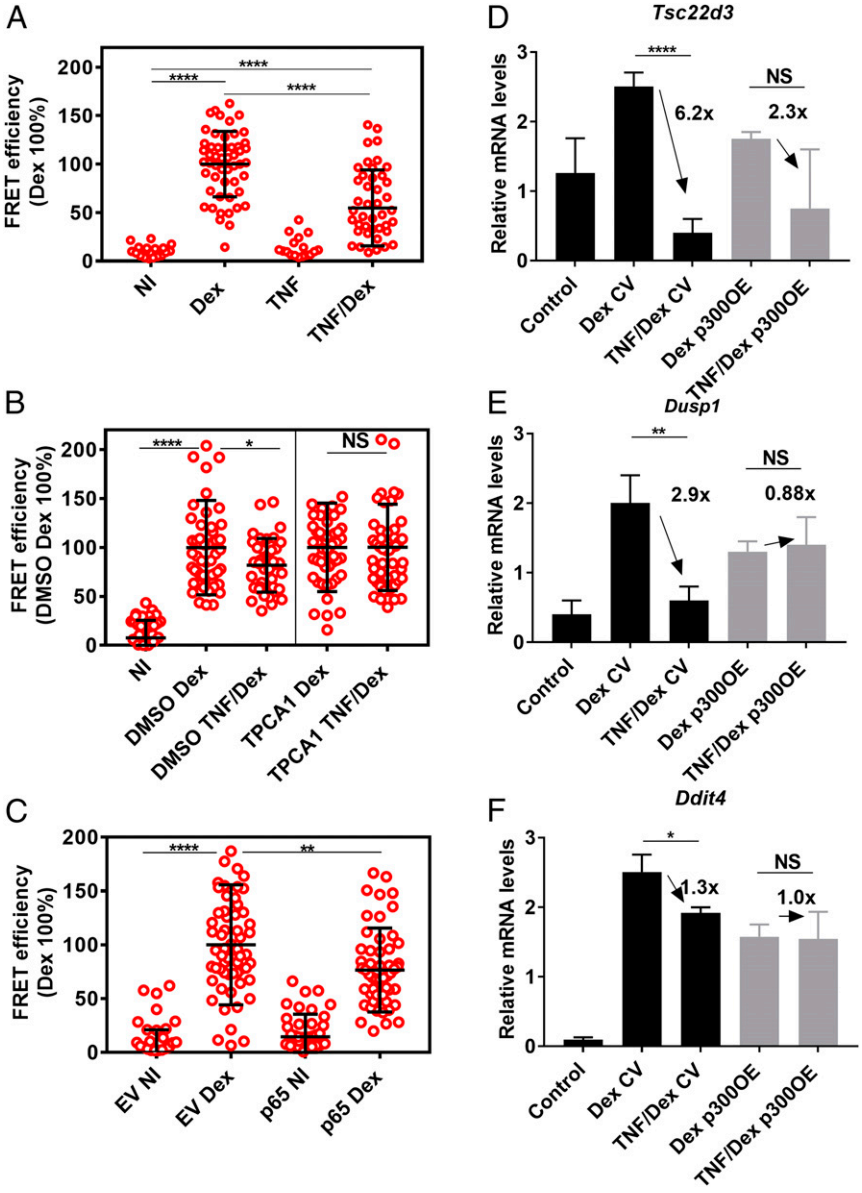

Fig. 5. GR and NFκB p65 interacted with p300 in cells depending on the stimulation and in vivo GCR can be prevented by p300. (*A*) FRET analysis of GR-p300 interaction in HEK293T cells transfected with ECFP-GR and EYFP-p300. Twenty-four hours after transfection, HEK293T cells were treated with Dex or with TNF/Dex, and FRET was measured 2 h after Dex addition. (*B*) The impact of 5 μM TPCA1, added 30 min before TNF on GR-p300 FRET. (*C*) Impact of cotransfection of a p65 expression plasmid on GR-p300 FRET. The normalized values were set as 100% for Dex and are shown as mean and SD (one-way ANOVA followed by Tukey's multiple comparisons test). (*D–F*) P300 was overexpressed in livers of mice via hydrodynamic tail vein injection. Shortly after high pressure injection, mice were injected with 30 μg of TNF, followed 6 h later with 100 μg of Dex injection. Hepatic *Tsc22d3*, *Dusp1*, and *Ddit4* mRNA was measured with qPCR and shown as the mean of the relative expression values ± SD ($n = 3$). Significances of P values are mentioned as $^*P < 0.05$, $^{**}P < 0.01$, $^{***}P < 0.001$, $^{****}P < 0.0001$, or NS (nonsignificant). CV, control vector.

(44). How it helps GR in activating transcription is less clear. It may acetylate GR itself, histones, or other proteins, leading to a change in the cofactor recruitment profile (45). Second, p300 has also been shown to function as a scaffold/docking platform for recruitment of other cofactors (46), and so a change in p300 interaction with a TF may cause a cascade of other differential bindings of other interacting proteins. Third, the extensive BioID experiment showed that p300 appeared significantly less associated to GR in TNF-pretreated cells (this study). Although we must be careful with the interpretation of this single experiment, the data were reproduced using FRET.

After treatment of cells with TNF and based on the HOMER motif analysis, the NFκB (mainly the p65 subunit)-binding sequence was dominantly enriched, suggesting that, in the BWTG3 RNA-Seq data, p65 is the major TNF-activated DNA-binding and p300-recruiting protein. Since NFκB activation appears to be sufficient to induce GCR and since the NFκB inhibitor TPCA1 reverted TNF-induced GCR, we suggest that, in conditions of TNF-induced GCR, the demand for p300 to provide both the GR and NFκB exceeded the supply, that NFκB became the dominant partner for p300 following a cofactor reshaping mechanism, and that p300 was recruited by the pathway that was first activated. Overexpression of p300 relieved this negative cross-talk and converted the balance back toward the GR-p300 axis and GR transcription-favoring pathways. The idea that p300 serves as a mediator for antagonistic cross-talk between various signaling pathways has been described for multiple TFs, such as NFκB versus HIF1α and others (47, 48).

The recruitment of CBP to GR upon TNF pretreatment, as found in the BioID study, can have an additional value in the establishment of TNF-induced GCR. Despite the fact that CBP and p300 are close homologs, opposing effects of CBP and p300 in GC signaling have been described in the past (49). Mounting the cofactor exchange model to the full, we might hypothesize that TNF pretreatment not only may recruit p300 to p65, resulting in reduced GR TA, but that, at the same time, that CBP may replace the p300 position on GR, leading to inhibition of the GR function even more. How these cofactor exchanges are regulated and whether both cofactors play an equally large share in the establishment of TNF-induced GCR needs to be investigated in more depth. This will have to be performed on a genome-wide perspective because older work, using GRE-luc reporter genes and overexpression studies, has shown the GR-inhibiting effects of p65, which was reverted by p300 but also by CBP (8).

Since both GR and NFκB are binding partners of p300, an exchange model between these TFs is a plausible model. Whether the reduction and new appearance of other GR-binding proteins under the influence of TNF are also to be explained by increased or decreased recruitment to other TFs, such as NFκB, or were a result of the p300 shuffle, or of posttranslational modifications of GR, is currently under investigation.

Overexpression of p300 seems an interesting strategy to overcome GCR. Since p300 is a cofactor that enhances both proinflammatory (NFκB) and antiinflammatory (GR) pathways, it may be a double-edged sword to be handled carefully. One might think to modify the interaction modality of p300 so GR is favored above p65. However, in-depth fine mapping of the interaction regions should be first considered. As far as we know, it has not been described whether GR and p65 interact at the same domain of p300. Another option is to interfere with the phosphorylation events that facilitate the interactions between p65 and p300, known to be regulated by protein kinase A (50), or the methylation by CARM1 that hinders the p300-GRIP1-NR complex formation (51). Since the BioID approach is not able to distinguish between direct or close indirect interactions, further studies are needed to characterize whether the interaction between GR and p300 involves GRIP1, which was also picked up with the BioID.

In conclusion, our studies about the impact of TNF on the direct GR gene up-regulation and down-regulation pathway revealed that TNF pretreatment obviously reshapes the GR interactome, which consequently results in reducing this type of GR transcriptional activity. P300 interaction was enriched at the GR after Dex stimulation, but not so, or much less, when the cells were pretreated with TNF. Because of the indispensable role for p300 in GR-dependent gene induction, we believe that TNF may abolish this GR function by recruiting p300 to the NFκB signaling pathway and that this leads to TNF-induced GCR. This reshuffling of p300 is not necessarily involved in other cases of GCR, however. Increasing the availability of p300 appears able to prevent the impact of TNF on GR transcriptional gene up-regulation and appears to be an interesting strategy to overcome TNF-induced GCR.

Materials and Methods

Cell Culture and Stimulations. A549 cells (human lung epithelial cells), BWTG3 cells (mouse hepatoma cells), and HEK293T cells (human embryonic kidney cells) were maintained and grown in Dulbecco's modified Eagle's medium (DMEM) (house-made) containing 10% FCS, 1 mM sodium pyruvate, 0.1 mM nonessential amino acids, and 2 mM L-glutamine. Before performing experiments, cells were starved for 24 h in Opti-MEM medium (Gibco, Invitrogen). Cells were then exposed to 1 μM Dex (Sigma, D-2915) and/or 1,000 U/mL recombinant TNF (produced in *Escherichia coli* and purified in our department) in Opti-MEM given 1 h before Dex stimulation. Unless otherwise indicated, cells were stimulated for 3 h in total. TPCA1 (2-[(aminocarbonyl)amino]-5-(4-fluorophenyl)-3-thiophenecarboxamide)/IKKb inhibitor) was obtained from Tocris Bioscience, and a stock dilution of 10^{-2} M was prepared in dimethyl sulfoxide (DMSO) and stored at −20 °C.

Mice, Injections, and Sampling. Female C57BL/6J mice were purchased from Janvier (Le Genest-St. Isle, France). Mice were housed in a temperature-controlled, air-conditioned animal house with 14-h and 10-h light/dark cycles and received food and water ad libitum. All mice were used at the age of 8 to 10 wk, and all experiments were approved by the institutional ethics committee for animal welfare of the Faculty of Sciences, Ghent University, Belgium. TNF and Rapidexon (Medini N.V.) were diluted in pyrogen-free PBS and injected intraperitoneally. P300 was overexpressed in mouse livers after hydrodynamic tail vein injection. Mice were injected in the tail vein over 5 s with the p300 plasmid solution (10 μg/mL in sterile, endotoxin-free PBS) in a volume equivalent to 10% of the body weight, as described (25). Twenty-four hours after transfection, mice were challenged with 30 μg of TNF given 6 h before 100 μg of Rapidexon. Livers were harvested 2 h after the last injection. For sampling liver tissue, mice were killed by cervical dislocation, and a piece of liver was harvested and stored in RNAlater (Qiagen) for RNA preparation.

Plasmids, Transfections, and Luciferase Reporter Assay. The plasmids p(GRE)2-50-luc and Kappab3luc (p(IL6κB)350hu.IL6-luc+), which have been described (8), were provided by K.D.B. CFP-tagged GR (pECFP-hGR) and YFP-tagged GR (pEYFP-GR) were provided by Ann Louw, University Stellenbosch, Stellenbosch, Republic of South Africa, and pFlag-p65, pFlag-IKKb, and hTRAF2-pLPCX-HA-Flag were provided by R.B. The human 6xHis-p300 plasmid (pcDNA3.1-p300) was purchased from Addgene. The pcDNA3-HA-IkappaBalpha-superrepressor was ordered at BCCM-LMBP (Ghent University, Ghent, Belgium). ON-TARGET plus Human EP300 siRNA (L-003486-00-0005) and ON-TARGET plus siCONTROL Nontargeting Pool (D-001810-10-20) were purchased from Dharmacon.

Concerning plasmids for FRET GR-p300 and p65-p300, genes coding for chimeric proteins for hGR-hp300 and hp65-hp300 FRET were cloned in the following vectors. The human p300 cDNA was cloned 3′ from the EYFP gene, in the pEYFP-C1 vector, thereby under control of the CMV-IE promoter and the SV40 polyA signal. Equally so, hGR and hp65 coding genes were cloned 3′ of the ECFP gene, in the pECFP-C1 vector, under control of the same CMV-IE promoter and the SV40 polyA signal. In all three cases, the start ATG codon of the p300, GR, and p65 coding genes was removed.

Lipofectamine LTX Reagent with PLUS Reagent (Invitrogen) was used to transiently transfect BWTG3 cells in 24-well plates, according to the manufacturer's instructions, whereas HEK293T cells were transfected according to the calcium phosphate transfection method. After 24 h, cells were treated with either 1 μM Dex and/or 1,000 U/mL TNF in Opti-MEM for the indicated durations. Cells were then harvested, and luciferase activity, expressed in arbitrary light units, was quantified with the Glomax instrument, measuring the D-luciferin (L-1349, Duchefa) conversion. Luciferase activity was corrected for the protein concentration in the sample by normalization to constitutive β-gal values. β-Gal levels were quantified with a chemiluminescent reporter assay, using Chlorophenol Red-β-D-galactosylpyranoside substrate.

Knockdown was performed in A549 cells using the Dharmafect siRNA transfection reagent following the manufacturer's manual. Cells were incubated for 72 h with siRNA before stimulation, harvesting, and RNA isolation.

Statistics. Data were expressed as means ± SEs of the means (SEM) in case the data were obtained from multiple independent experiments and as means ± SD if the data were derived from a single experiment. Statistical significance was evaluated with Student's *t* test and one-way or two-way ANOVA in GraphPad Prism 7.0 software (GraphPad Software, San Diego, CA). Fold changes or ratios were log (Y) transformed before statistical analysis. If applicable, post hoc analysis was performed using the Tukey's test, to correct for multiple testing during the pairwise multiple comparisons or the Dunnett's analysis to compare different conditions to one control group. The symbols *, **, ***, and **** represent $P < 0.05$, $P < 0.01$, $P < 0.001$, and $P < 0.0001$, respectively.

For RNA isolation and qPCR, RNA sequencing, Western blot analysis, dot blot, immunofluorescence, fluorescence resonance energy transfer (FRET), fluorescence lifetime imaging microscopy (FLIM), Chip qPCR and sequencing, peak calling and motif discovery, BirA BioID technology, preparation for mass spectrometry, quantitative liquid chromatography–mass spectrometry, and protein identification, see *SI Appendix, Supporting Information Methods*.

ACKNOWLEDGMENTS. We thank Lode De Cauwer for generating and providing us with the A549-GRE-luc cells. We acknowledge Prof. Dr. Marnik Vuylsteke for statistical assistance. We thank the Vlaams Instituut voor Biotechnologie (VIB) sequencing core facility for performing the RNA sequencing and ChIP-Seq; and the VIB imaging core facility for performing all microscopy work for the FRET experiments. We thank Adjunct Professor Markku Varjosalo, head of the proteomics unit of the University of Helsinki, for performing the mass spectrometry analysis of the BioID experiment.

1. M. A. Lazar, Maturing of the nuclear receptor family. *J. Clin. Invest.* **127**, 1123–1125 (2017).
2. P. J. Barnes, Glucocorticosteroids: Current and future directions. *Br. J. Pharmacol.* **163**, 29–43 (2011).
3. B. O'Malley, The steroid receptor superfamily: More excitement predicted for the future. *Mol. Endocrinol.* **4**, 363–369 (1990).
4. S. Vandevyver, L. Dejager, C. Libert, On the trail of the glucocorticoid receptor: Into the nucleus and back. *Traffic* **13**, 364–374 (2012).
5. S. Vandevyver, L. Dejager, J. Tuckermann, C. Libert, New insights into the anti-inflammatory mechanisms of glucocorticoids: An emerging role for glucocorticoid-receptor-mediated transactivation. *Endocrinology* **154**, 993–1007 (2013).
6. B. J. Schiller, R. Chodankar, L. C. Watson, M. R. Stallcup, K. R. Yamamoto, Glucocorticoid receptor binds half sites as a monomer and regulates specific target genes. *Genome Biol.* **15**, 418 (2014).
7. H. M. Reichardt *et al*., DNA binding of the glucocorticoid receptor is not essential for survival. *Cell* **93**, 531–541 (1998).
8. K. De Bosscher *et al*., Glucocorticoids repress NF-kappaB-driven genes by disturbing the interaction of p65 with the basal transcription machinery, irrespective of coactivator levels in the cell. *Proc. Natl. Acad. Sci. U.S.A.* **97**, 3919–3924 (2000).
9. M. Surjit *et al*., Widespread negative response elements mediate direct repression by agonist-liganded glucocorticoid receptor. *Cell* **145**, 224–241 (2011).
10. M. Ballegeer *et al*., Glucocorticoid receptor dimers control intestinal STAT1 and TNF-induced inflammation in mice. *J. Clin. Invest.* **128**, 3265–3279 (2018).
11. J. Xu, Q. Li, Review of the in vivo functions of the p160 steroid receptor coactivator family. *Mol. Endocrinol.* **17**, 1681–1692 (2003).
12. C. J. Fryer, T. K. Archer, Chromatin remodelling by the glucocorticoid receptor requires the BRG1 complex. *Nature* **393**, 88–91 (1998).
13. A. K. McDonough, J. R. Curtis, K. G. Saag, The epidemiology of glucocorticoid-associated adverse events. *Curr. Opin. Rheumatol.* **20**, 131–137 (2008).
14. P. J. Barnes, I. M. Adcock, Glucocorticoid resistance in inflammatory diseases. *Lancet* **373**, 1905–1917 (2009).
15. K. Dendoncker, C. Libert, Glucocorticoid resistance as a major drive in sepsis pathology. *Cytokine Growth Factor Rev.* **35**, 85–96 (2017).
16. L. Dejager, S. Vandevyver, I. Petta, C. Libert, Dominance of the strongest: Inflammatory cytokines versus glucocorticoids. *Cytokine Growth Factor Rev.* **25**, 21–33 (2014).
17. R. M. Locksley, N. Killeen, M. J. Lenardo, The TNF and TNF receptor superfamilies: Integrating mammalian biology. *Cell* **104**, 487–501 (2001).
18. M. Krishna, H. Narang, The complexity of mitogen-activated protein kinases (MAPKs) made simple. *Cell. Mol. Life Sci.* **65**, 3525–3544 (2008).
19. G. Natoli *et al*., Activation of SAPK/JNK by TNF receptor 1 through a noncytotoxic TRAF2-dependent pathway. *Science* **275**, 200–203 (1997).
20. S. Yamaoka *et al*., Complementation cloning of NEMO, a component of the IkappaB kinase complex essential for NF-kappaB activation. *Cell* **93**, 1231–1240 (1998).
21. C. Libert *et al*., Response of interleukin-6-deficient mice to tumor necrosis factor-induced metabolic changes and lethality. *Eur. J. Immunol.* **24**, 2237–2242 (1994).
22. L. Dejager *et al*., Neutralizing TNFα restores glucocorticoid sensitivity in a mouse model of neutrophilic airway inflammation. *Mucosal Immunol.* **8**, 1212–1225 (2015).
23. T. Kino, G. P. Chrousos, Tumor necrosis factor α receptor- and Fas-associated FLASH inhibit transcriptional activity of the glucocorticoid receptor by binding to and interfering with its interaction with p160 type nuclear receptor coactivators. *J. Biol. Chem.* **278**, 3023–3029 (2003).
24. T. Van Bogaert, K. De Bosscher, C. Libert, Crosstalk between TNF and glucocorticoid receptor signaling pathways. *Cytokine Growth Factor Rev.* **21**, 275–286 (2010).
25. T. Van Bogaert *et al*., Tumor necrosis factor inhibits glucocorticoid receptor function in mice: A strong signal toward lethal shock. *J. Biol. Chem.* **286**, 26555–26567 (2011).
26. G. J. Zijlstra, N. H. Ten Hacken, R. F. Hoffmann, A. J. van Oosterhout, I. H. Heijink, Interleukin-17A induces glucocorticoid insensitivity in human bronchial epithelial cells. *Eur. Respir. J.* **39**, 439–445 (2012).
27. K. Dendoncker *et al*., TNF induces glucocorticoid resistance by reshaping the GR nuclear cofactor profile: Investigation of TNF mediated effects on the GR mediated gene expression. Gene Expression Omnibus. https://www.ncbi.nlm.nih.gov/geo/query/acc.cgi?acc=GSE124088. Deposited 19 December 2018.
28. S. Vandevyver *et al*., Glucocorticoid receptor dimerization induces MKP1 to protect against TNF-induced inflammation. *J. Clin. Invest.* **122**, 2130–2140 (2012).
29. K. Dendoncker *et al*.,TNF induces glucocorticoid resistance by reshaping the GR nuclear cofactor profile: Investigation of TNF mediated effects on the GR-DNA binding. Gene Expression Omnibus. https://www.ncbi.nlm.nih.gov/geo/query/acc.cgi?acc=GSE123953. Deposited 17 December 2018.
30. R. Varnaitė, S. A. MacNeill, Meet the neighbors: Mapping local protein interactomes by proximity-dependent labeling with BioID. *Proteomics* **16**, 2503–2518 (2016).
31. J. K. Lempiäinen *et al*., Agonist-specific protein interactomes of glucocorticoid and androgen receptor as revealed by proximity mapping. *Mol. Cell. Proteomics* **16**, 1462–1474 (2017).
32. D. Mellacheruvu *et al*., The CRAPome: A contaminant repository for affinity purification-mass spectrometry data. *Nat. Methods* **10**, 730–736 (2013).
33. D. Bittencourt *et al*., G9a functions as a molecular scaffold for assembly of transcriptional coactivators on a subset of glucocorticoid receptor target genes. *Proc. Natl. Acad. Sci. U.S.A.* **109**, 19673–19678 (2012).
34. Q. Li, A. Su, J. Chen, Y. A. Lefebvre, R. J. G. Haché, Attenuation of glucocorticoid signaling through targeted degradation of p300 via the 26S proteasome pathway. *Mol. Endocrinol.* **16**, 2819–2827 (2002).
35. K. De Bosscher, W. Vanden Berghe, G. Haegeman, The interplay between the glucocorticoid receptor and nuclear factor-kappaB or activator protein-1: Molecular mechanisms for gene repression. *Endocr. Rev.* **24**, 488–522 (2003).
36. L. F. Chen, Y. Mu, W. C. Greene, Acetylation of RelA at discrete sites regulates distinct nuclear functions of NF-kappaB. *EMBO J.* **21**, 6539–6548 (2002).
37. R. J. Farrell, D. Kelleher, Glucocorticoid resistance in inflammatory bowel disease. *J. Endocrinol.* **178**, 339–346 (2003).
38. F. Van Hauwermeiren, R. E. Vandenbroucke, C. Libert, Treatment of TNF mediated diseases by selective inhibition of soluble TNF or TNFR1. *Cytokine Growth Factor Rev.* **22**, 311–319 (2011).
39. F. Van Hauwermeiren *et al*., TNFR1-induced lethal inflammation is mediated by goblet and Paneth cell dysfunction. *Mucosal Immunol.* **8**, 828–840 (2015).
40. C. Brightling, M. Berry, Y. Amrani, Targeting TNF-alpha: A novel therapeutic approach for asthma. *J. Allergy Clin. Immunol.* **121**, 5–10, quiz 11–12 (2008).
41. A. Y. So, C. Chaivorapol, E. C. Bolton, H. Li, K. R. Yamamoto, Determinants of cell- and gene-specific transcriptional regulation by the glucocorticoid receptor. *PLoS Genet.* **3**, e94 (2007).
42. R. Bhandare *et al*., Glucocorticoid receptor interacting protein-1 restores glucocorticoid responsiveness in steroid-resistant airway structural cells. *Am. J. Respir. Cell Mol. Biol.* **42**, 9–15 (2010).
43. D. C. Bedford, P. K. Brindle, Is histone acetylation the most important physiological function for CBP and p300? *Aging (Albany N.Y.)* **4**, 247–255 (2012).
44. S. P. Mukherjee *et al*., Analysis of the RelA:CBP/p300 interaction reveals its involvement in NF-κB-driven transcription. *PLoS Biol.* **11**, e1001647 (2013).
45. B. Guo, X. Huang, S. Cooper, H. E. Broxmeyer, Glucocorticoid hormone-induced chromatin remodeling enhances human hematopoietic stem cell homing and engraftment. *Nat. Med.* **23**, 424–428 (2017).
46. B. L. Conway-Campbell *et al*., The HSP90 molecular chaperone cycle regulates cyclical transcriptional dynamics of the glucocorticoid receptor and its coregulatory molecules CBP/p300 during ultradian ligand treatment. *Mol. Endocrinol.* **25**, 944–954 (2011).
47. D. B. Mendonça, G. Mendonça, F. J. Aragão, L. F. Cooper, NF-κB suppresses HIF-1α response by competing for P300 binding. *Biochem. Biophys. Res. Commun.* **404**, 997–1003 (2011).
48. R. H. Kim *et al*., SNIP1 inhibits NF-kappa B signaling by competing for its binding to the C/H1 domain of CBP/p300 transcriptional co-activators. *J. Biol. Chem.* **276**, 46297–46304 (2001).
49. C. Fonte, A. Trousson, J. Grenier, M. Schumacher, C. Massaad, Opposite effects of CBP and p300 in glucocorticoid signaling in astrocytes. *J. Steroid Biochem. Mol. Biol.* **104**, 220–227 (2007).
50. H. Zhong, R. E. Voll, S. Ghosh, Phosphorylation of NF-kappa B p65 by PKA stimulates transcriptional activity by promoting a novel bivalent interaction with the coactivator CBP/p300. *Mol. Cell* **1**, 661–671 (1998).
51. Y. H. Lee, S. A. Coonrod, W. L. Kraus, M. A. Jelinek, M. R. Stallcup, Regulation of coactivator complex assembly and function by protein arginine methylation and demethylimination. *Proc. Natl. Acad. Sci. U.S.A.* **102**, 3611–3616 (2005).